Toward Optimizing Coarse Aggregate Types and Sizes in High-strength Concrete

Madeh I. Hamakareem[1†], Daban A. Muhedin[2], Ahmed J. Hama Rash[1], Sangar J. Qadir[3], and Loghman Khodakarami[4]

[1]Department of Geotechnical Engineering, Faculty of Engineering, Koya University, Koya KOY45, Kurdistan Region-F.R, Iraq

[2]Department of Civil Engineering, Faculty of Engineering, Koya University, Koya KOY45, Kurdistan Region-F.R, Iraq

[3]Department of Civil Engineering, College of Engineering, University of Sulaimani, Sulaimani, Kurdistan Region-F.R, Iraq

[4]Department of Petroleum Engineering, Faculty of Engineering, Koya University, Koya KOY45, Kurdistan Region-F.R, Iraq

***Abstract*—The development of very effective coarse aggregate types and sizes can lead to a rapid increase in the production of high strength concrete (HSC). This research investigates the effects of five different coarse aggregate types and a range of maximum coarse aggregate sizes on the mechanical properties of concrete through experimental tests and numerical analysis. The workability of fresh concrete is examined using the slump cone test, whereas the mechanical performance of hardened concrete is assessed through compressive strength and splitting tensile strength tests. The experimental results are compared to the predicted results from the codes and design guidelines to assess their predictions. Both coarse aggregate types and sizes show a significant influence on the mechanical properties of HSC performance, especially the compressive strength of HSC, which could be increased on average by 25%. Moreover, the predictions of splitting tensile strength using the ACI 318 and ACI 363 equations are not very accurate, particularly at a high strength range. Therefore, this study develops a new equation for predicting splitting tensile strength based on both experimental test results conducted in this research and a significant amount of data collected from the literature. Evaluation metrics, including R2, RMSE, MAPE, and MAE, demonstrate the superior accuracy of the proposed equation compared to the design guidelines equations. The findings of this research can contribute toward the optimization of aggregate type and size in concrete mix design for enhanced performance and provide valuable insights into the relationship between compressive and splitting tensile strengths in HSC.**

***Index Terms*—High-strength concrete, maximum aggregate size, compressive strength, splitting tensile strength, aggregate types**

ARO-The Scientific Journal of Koya University
Vol. XII, No.2 (2024), Article ID: ARO.11589. 11 pages
Doi: 10.14500/aro.11589
Received: 28 March 2024; Accepted: 26 June 2024
Regular research paper; Published: 25 July 2024
[†]Corresponding author's e-mail: madeh.izat@koyauniversity.org

I. Introduction

High-strength concrete (HSC) has been used widely throughout the world, but its popularity has recently emerged in Iraq. It is defined as concrete with a compressive strength of 55 MPa or greater (ACI Committee 363, 2010). HSC production utilizes common materials such as cement, sand, and coarse aggregate, along with admixtures such as high-range water-reducing admixture, silica fume, and fly ash (Darwin and Dolan, 2021). However, achieving desired strength relies on a low water-to-cement ratio (Wu et al., 2001b) and strict quality control during production (Darwin and Dolan, 2021). The application of HSC is driven by its high uniform density, low permeability, and high durability. It has been used in the columns of high-rise buildings to reduce size, increase floor space, and permit longer spans in bridges (Gjørv, 2008; ACI Committee 363, 2010).

The properties of HSC, and in particular compressive strength, which is one of the most significant criteria in the design of concrete structures, are influenced by parameters, namely: Cement type, supplementary cementitious materials, chemical admixtures, and curing regimes. However, the properties of coarse aggregate, especially its types and maximum particle size, significantly impact the strength behavior of HSC (Caldarone, 2009; Meddah, Zitouni and Belâabes 2010; Jin et al., 2021). The role of coarse aggregate in compressive strength is critical in HSC. This is due to the high matrix strength in HSC, which increases the likelihood of crack development through aggregates and consequently modifies cracking mechanisms compared to ordinary concrete (Neville and Brooks, 2010).

The relationship between maximum coarse aggregate size (MCAS) and the compressive strength of HSC has been studied by many researchers. For instance, Wu, Chen and Yao (2001a) reported that the compressive strength of HSC increases as MCAS increases but subsequently decreases beyond MCAS of 15 mm. Experimental investigations

http://dx.doi.org/10.14500/aro.11589

conducted by Rao and Prasad (2002) and Akçaoğlu, Tokyay and Çelik (2002) emphasized a positive correlation between MCAS and compressive strength, with peak strength observed at a MCAS of 20 mm and 32 mm, respectively.

However, Meddah, Zitouni and Belâabes (2010) observed only a marginal increase in the compressive strength of HSC when MCAS was reduced from 25 mm to 15 mm. Moreover, Grabiec, Zawal and Szulc (2015) conducted a study to examine the influence of MCAS (8 mm and 16 mm), aggregate type (gravel, crushed basalt, and crushed granite), and cement content (600 kg/m^3 and 700 kg/m^3) on the properties of HSC. They found that reducing MCAS increased compressive strength for both gravel and crushed granite but led to a significant reduction for crushed basalt at 700 kg/m^3 cement content. At lower cement content, decreasing MCAS reduced compressive strength for gravel and crushed granite but improved it for crushed basalt. They also acknowledge that a wider range of MCAS needs to be explored to specify the relationship between aggregate size and the strength behavior of HSC. A more recent numerical and theoretical investigation by Jin et al. (2021) showed that the strength of concrete roughly increased as the MCAS was reduced. MCAS is also found to influence the tensile strength of HSC. According to studies conducted by Akçaoğlu, Tokyay and Çelik (2002) and Al-Oraimi, Taha and Hassan (2006), the tensile strength of HSC increases with decreasing MCAS, whereas Rao and Prasad (2002) reported the opposite trend. These conflicting results highlight the need for further investigation to clarify the effects of MCAS on the compressive strength and tensile strength of HSC.

Several researchers (Kılıç et al., 2008; Beushausen and Dittmer, 2015; Vishalakshi, Revathi and Sivamurthy Reddy 2018) have identified aggregate type (strength, shape, surface texture, and mineralogy) as a critical factor affecting the compressive strength of HSC. Their findings indicate that stronger aggregates contribute to an overall enhancement in the strength of concrete. Moreover, these studies reveal a similar relationship between aggregate strength and the splitting tensile strength of concrete. However, Beushausen and Dittmer (2015) reported that the effect of aggregate strength on the splitting tensile strength or flexural strength of concrete is limited. The investigation conducted by Grabiec, Zawal and Szulc (2015) provided valuable insights into the factors affecting the compressive strength of HSC, but it did not reach conclusive findings regarding the sole influence of the aggregate type. In their study, Góra and Piasta (2020) investigated the impact of six distinct types of coarse aggregates on the properties of both ordinary and high-performance concrete. The experimental results revealed that an increase in aggregate strength does not always result in a corresponding increase in the compressive strength or splitting tensile strength of high-performance concrete. These mixed findings underscore the complexity and the need for further exploration of the influence of coarse aggregate characteristics on the strength behavior of HSC.

As discussed above, the influence of MCAS size and coarse aggregate type on the compressive strength and splitting tensile strength of HSC concrete remains inconsistent across various studies. Moreover, research on producing HSC without supplementary cementitious materials is also limited. In addition, previous investigations lack consensus regarding the optimum aggregate size and type for producing HSC. Thus, our research aims to systematically investigate the effects of five coarse aggregate types (crushed gravel [CG], crushed limestone [CL], crushed dolomitic limestone [DL], crushed high-calcium limestone [HCL], and natural gravel [NG]) and various MCAS (9.5 mm, 12.5 mm, 19 mm, and 25 mm) for CG on the compressive strength and splitting tensile strength of HSC. We seek to provide clearer insights into optimizing aggregate type and size in concrete mix for enhanced performance and contribute to the development of a more sustainable and potentially more cost-effective production of HSC. By combining experimental tests with numerical analysis, this study also aims to improve an equation based on existing ACI 363R-10 and ACI 319-14 equations for predicting splitting tensile strength based on the compressive strength of HSC.

II. Experimental Program

A. Materials and Test Methods

Ordinary Portland Cement (Type I) was consistently used in this investigation for all mixtures. A liquid polycarboxylic-based superplasticizer was utilized in this work to reduce mixing water and maintain concrete workability. Natural river sand with a smooth surface and rounded-shaped particles was used as fine aggregate. Its specific gravity and water absorption, determined based on ASTM C128-15 (2015), were 2.7 and 0.6%, respectively. The grading of fine aggregate complied with ASTM C 33/C33M-18 (2018), see Fig. 1.

In this experimental investigation, five different aggregate types, namely: CG, CL, DL, HCL, and NG, were utilized to examine the effect of aggregate types on the strength behavior of HSC. The aggregates were sourced from three different aggregate production plants within the Sulaymaniyah governorate/Iraq, see Fig. 2a.

The types of aggregates were identified using macroscopic observation and X-ray fluorescence (XRF) testing. The results of XRF tests for the five types of aggregates are presented

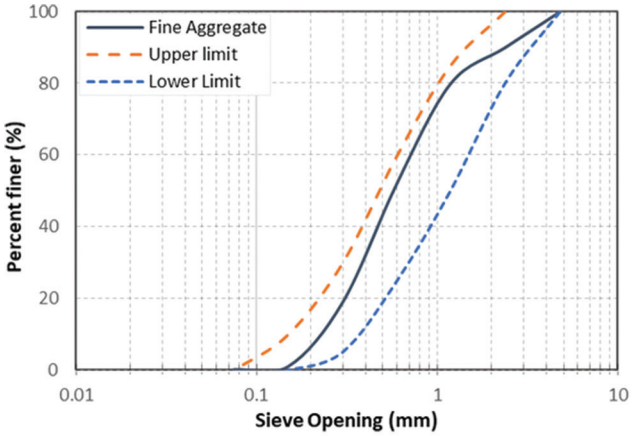

Fig. 1. Particle size distribution of fine aggregate.

Fig. 2. (a) Aggregate plant locations with respective aggregate types in brackets, (b) Coarse aggregate types: (a) crushed gravel, (b) crushed limestone, (c) crushed dolomitic limestone, (d) crushed high-calcium limestone, and (e) natural gravel.

in Table I. Visual observation showed that CG aggregate contained limited proportions of uncrushed particles and a small percentage of limestone aggregates. We conducted visual assessments on CG samples and differentiated between uncrushed and limestone particles. The separated particles were weighted differently, and the average percentage of different components was computed. The rationale behind using this technique was to determine major components quickly. The detailed physical characteristics of different coarse aggregates are summarized in Table II. To investigate the influence of MCAS on the compressive strength and splitting tensile strength of HSC, CG aggregates with different MCAS of 9.5 mm, 12.5 mm, 19 mm, and 25 mm were used.

In the selection of aggregate types and sizes, we prioritized local availability to reduce transportation impacts and costs. Not only does this strategy support the local economy, but it is also in line with environmental standards aimed at reducing carbon footprints related to construction materials. In addition, our choices met the requirements of relevant standards like ASTM C 33 for aggregates, which offer guidelines on the grading and quality of aggregates. Particle size analysis of various aggregate types and different sizes of CG considered in this study conformed to the requirements of ASTM C 33/C33M-18 (2018), as shown in TABLE III and presented graphically in Fig. 3. ACI 363R-10 sets ASTM C33 as the minimum requirement for aggregate to produce HSC.

B. Mix Proportions and Sample Preparation

The concrete mixture was designed following the guidelines outlined in ACI Committee 211 (2008) and was

TABLE I
Results of X-ray Fluorescence (XRF) of Different Types of Coarse Aggregate, %

Aggregate types	CaO	SiO_2	Al_2O_3	MgO	Fe_2O_3	Others
Crushed gravel	16.20	70.51	6.89	0.98	2.60	2.82
Crushed limestone	67.42	19.75	4.96	3.76	1.85	2.26
Crushed dolomitic limestone	81.46	4.10	1.79	10.42	0.70	1.53
Crushed high-calcium limestone	83.07	8.69	4.21	1.43	0.95	1.63
Natural gravel	5.12	77.93	12.64	0.88	1.55	1.88

further refined through the use of trial mixes. The proportion of the mixture for all concrete specimens remained consistent throughout the experimental program and consisted of 560 kg/m^3 of cement, 175 kg/m^3 of water, 660 kg/m^3 of sand, 1027 kg/m^3 of coarse aggregate, and 4.48 kg/m^3 of superplasticizer. The concrete constituents were thoroughly mixed in a tilted concrete mixer, Fig. 4a. Initially, the coarse aggregate and a portion of the mixing water are blended. Then, sand, cement, and approximately 70% of the water are added to the mixer incrementally and mixed for about 5 min. Subsequently, the remaining water is combined with the superplasticizer and introduced into the mixture, followed by an additional 5 min of mixing.

After the mixing process, a slump test was conducted in accordance with ASTM C143/C143M−15a (2015) to assess the workability of fresh concrete. Standard steel cylinders with a diameter of 100 mm and a height of 200 mm were oiled, poured in three layers, and adequately compacted using a table vibrator, Fig. 4b.

The concrete specimens cast, as shown in Fig. 4c, for the assessment of both compressive strength and splitting tensile strength were moist-cured and tested after 7, 28, and 56 days.

 http://dx.doi.org/10.14500/aro.11589

TABLE II
PHYSICAL PROPERTIES OF DIFFERENT COARSE AGGREGATES (CG, CL, DL, HCL, AND NG)

Properties of aggregate	CG	CL	DL	HCL	NG	Standards
Specific Gravity	2.68	2.72	2.71	2.50	2.65	(ASTM C127-15, 2015)
Water Absorption, %	1.22	0.8	1.0	1.72	1.46	(ASTM C127-15, 2015)
Flakiness and Elongation Index, %	7.1	7.8	9.3	8	6.6	(ASTM D4791–10, 2010)
Impact value, %	5.7	6.9	7.1	12.1	4.9	(BS 812-112:1990, 1990)
Unit weight, kg/m^3	1600	1590	1530	1560	1600	(ASTM C29/C29M-17a, 2017)
Surface Texture	Mostly Rough	Rough	Rough	Rough	Smooth	-

CG: Crushed gravel, CL: Crushed limestone, DL: Dolomitic limestone, HCL: High-calcium limestone, NG: Natural gravel

TABLE III
PARTICLE SIZE ANALYSIS OF DIFFERENT AGGREGATE SIZES OF CG AND AGGREGATE TYPES (CG, CL, DL, HCL, AND NG) AS PER ASTM C136/C136M-14 (2014)

Aggregate type	CG	CG	CG	CG	CL	DL	HCL	NG
Aggregate size, mm	25	19	12.5	9.5	12.5	12.5	12.5	12.5
% Passing 25 mm	100	-	-	-	-	-	-	-
% Passing 19 mm	67.45	100	-	-	-	-	-	-
% Passing 12.5 mm	20.41	40.77	97.5	-	100	98.9	100	97
% Passing 9.5 mm	5.34	7.34	40.4	100	44.5	45.4	69.7	65.8
% Passing 4.75 mm		0.06	13.1	19	11.2	0.7	14.60	2.5
% Passing 2.36 mm	-	-	0	4.6	1.4	0	0.49	0.1
% Passing 1.18 mm	-	-	-	2	-	-	-	-

CG: Crushed gravel, CL: Crushed limestone, DL: Dolomitic limestone, HCL: High-calcium limestone, NG: Natural gravel

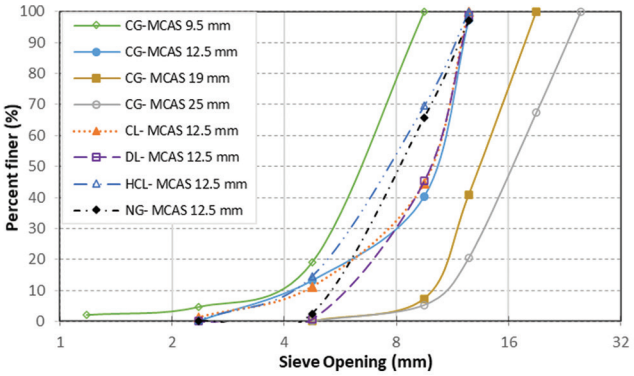

Fig. 3. Particle size distribution of different coarse aggregates.

A total of three specimens were formulated for each compressive strength and splitting tensile strength reading. The compression test was conducted based on ASTM C39/C39M-14 (2018) (Fig. 4d), whereas the splitting tensile test was carried out according to ASTM C496/C496M-11 (2011) (Fig. 4e).

III. RESULTS AND DISCUSSIONS

A. Workability

The influence of MCAS on concrete workability, as indicated by the slump value, is illustrated in Fig. 5a. It can be observed that the workability of concrete increased with an increase in MCAS. For instance, concrete produced with a 9.5 mm MCAS obtained the lowest slump value (200 mm), whereas concrete made with a 25 mm MCAS yielded the highest slump value (230 mm). This effect is attributed to the larger particles, which result in a smaller surface area for a given amount of aggregate mass, thereby reducing the water demand in a concrete mixture (Neville, 2011).

Fig. 5b demonstrates how aggregate types affect the workability of concrete in terms of slump value. The slump values of CG, CL, and DL concrete were similar and smaller when compared to the slump value of NG concrete. This is because the former concrete series was produced from angular, rough-surfaced, crushed aggregate, whereas the latter was produced from rounded and smooth-surfaced natural aggregate.

It was noticed that HCL concrete, despite sharing a similar shape and surface texture aggregates with CG, CL, and DL concrete, exhibited a lower slump value than its counterparts. This can be attributed to the aggregate gradation of HCL aggregate, which contained a higher proportion of smaller particles when contrasted with CG, CL, and DL aggregate, see Table III. This observation is supported by the test results reported by Uddin et al. (2017). Higher water absorption of HCL aggregate, as presented in Table I, could also contribute to the reduction of slump in HCL aggregate concrete.

Increasing MCAS improves workability, benefiting concrete placement and consolidation. However, this improvement comes at the cost of reducing compressive strength. To quantify this trade-off, this study explored the effect of MCAS on the compressive strength of HSC. For instance, both 9.5 mm and 12.5 mm MCAS yielded slump values of 200 mm and 215 mm, respectively. However, the 9.5 mm mix achieved a higher compressive strength of 67.07 MPa compared to the 60.56 MPa of the 12.5 mm mix. In addition, a 25 mm mix produced a slump value of 230, but compressive strength dropped to 50.01 MPa, which is not considered HSC. This highlights the significance of optimizing HSC mix design to ensure efficient construction and structural performance.

B. Compressive Strength

Coarse aggregate is a crucial parameter that affects the compressive strength of HSC. The compressive strength results of concrete specimens containing different coarse aggregate types (CG, CL, DL, HCL, and NG) and moist-cured for 7, 28, and 56 days are presented in Fig. 6.

Fig. 6 shows a significant variation in compressive strength among different aggregate types, highlighting the important role of aggregate characteristics (strength, shape, surface texture, and mineralogy) in determining the compressive strength of HSC. At 7 days of curing, the compressive strength of CG concrete was 1.2%, 13.2%, 17.3%, and

Fig. 4. (a) concrete mixer, (b) shaking table, (c) some of the cast samples, (d) compression testing, and (e) splitting tensile testing.

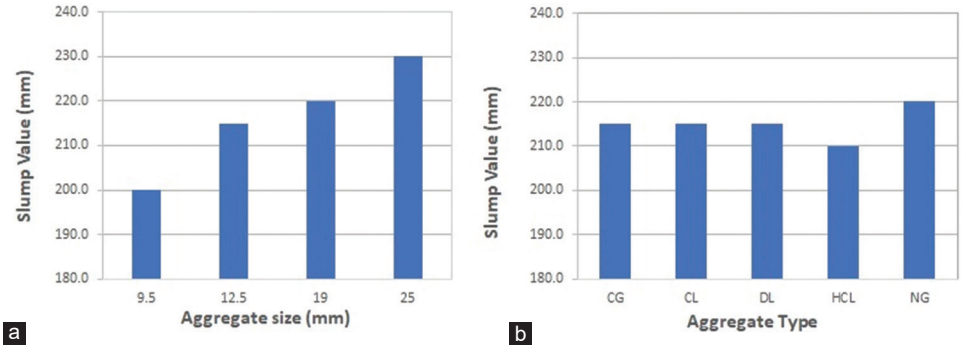

Fig. 5. Effect of (a) maximum coarse aggregate size, (b) aggregate type on concrete workability.

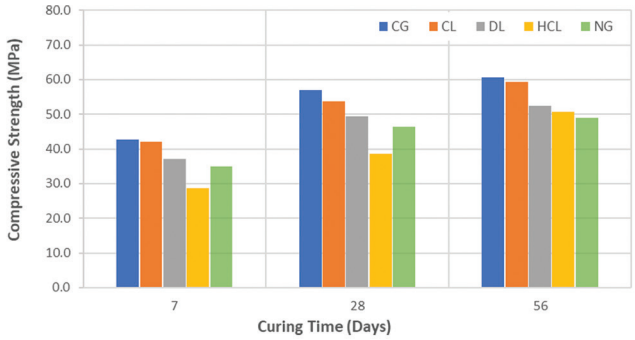

Fig. 6. Influence of different aggregate types on the compressive strength of HSC.

32.6% higher compared to CL, DL, NG, and HCL concrete, respectively. Similarly, at 28 days of curing, the CG concrete exhibited a 5.7% higher compressive strength compared to CL concrete, 13.3% higher than DL concrete, 18.56% higher than NG concrete, and 32.32% higher than HCL concrete. At 56 days of curing, CG concrete achieved the highest compressive strength, measuring 60.56 MPa, surpassing CL, DL, HCL, and NG concrete by 2.1%, 13.3%, 16.1%, and 19.1%, respectively.

Despite having similar surface textures and a maximum aggregate size of 12.5 mm for the crushed aggregates, CG concrete consistently exhibited the highest compressive strength throughout all curing periods. CL concrete showed comparable compressive strength to CG concrete but was significantly higher compared to DL and HCL concrete. These variations are attributed to the differing strength characteristics and mineralogy of the crushed aggregates. The physical properties of the aggregates, as presented in Table II, indicate a stronger nature of CG and CL aggregates in comparison to DL and HCL aggregates. Moreover, the XRF test results in Table I reveal that CG and CL aggregates contain a higher proportion of quartz minerals compared to other crushed aggregates, and such aggregates generally demonstrate better mechanical properties (Liu et al., 2005). On the other hand, DL and HCL aggregates contain a significant amount of calcite minerals, as indicated in Table I. The presence of calcite minerals in these aggregates contributes to their inferior mechanical properties, as

evidenced by test results reported by Beshr, Almusallam and Maslehuddin (2003).

NG concrete showed the lowest compressive strength at 56 days of curing, which can be related to a smooth surface and rounded gravel particles, resulting in a reduced aggregate-cement paste bonding strength. The compressive strength of NG concrete was higher compared to HCL concrete after 7 and 28 days, but HCL concrete exhibited greater strength after 56 days. This reversal might be due to strong bonding strength at the HCL-cement paste interface at a high strength level.

Fig. 7 shows the failure of tested specimens, made from different aggregates, after compression tests. Cracks predominantly passed through aggregates in CG and CL concretes, indicating a good aggregate-cement paste bond (Fig. 7a and b). However, a few instances of debonding between uncrushed particles and cement paste were observed in CG concrete (Fig. 7a), highlighting the impact of aggregate surface texture on the interfacial bond. Both DL and HCL concrete exhibited similar failure patterns, with cracks propagating through the middle of the specimens from top to bottom (Fig. 7c and d). Despite comparable surface textures, DL concrete achieved higher compressive strength than HCL concrete, underscoring the role of aggregate strength in enhancing overall strength in HSC. The NG specimen showed sporadic cracks throughout its height (Fig. 7e), possibly indicating localized failure due to a weak interfacial bond, likely related to the smooth surface texture of the NG aggregate.

Fig. 8 illustrates the compressive strength of concrete made from CG with varying MCAS of 9.5 mm, 12.5 mm, 19 mm, and 25 mm, and moisture-cured for 7, 28, and 56 days. It is evident that the compressive strength results are influenced by MCAS and curing time. The compressive strength of cylinder specimens increased as the MCAS increased.

At 7 days of curing, the compressive strength of concrete with an MCAS of 9.5 mm was 48.01 MPa. In comparison, for concretes made with MCAS of 12.5 mm, 19 mm, and 25 mm, the corresponding strengths were 42.66 MPa, 35.86 MPa, and 30.29 MPa, respectively. At 28 days, the compressive strength of concrete made with MCAS of 9.5 mm, 12.5 mm, 19 mm, and 25 mm was 61.09 MPa, 56.93 MPa, 45.84 MPa, and 40.77 MPa, respectively.

For the 56-day curing period, concrete formulated with MCAS of 9.5 mm and 12.5 mm achieved compressive strengths of 67.07 MPa and 60.56 MPa, respectively. In contrast, the concrete specimens produced using MCAS of 19 mm and 25 mm demonstrated compressive strengths of 50.75 MPa and 50.21 MPa, respectively, falling short of the HSC criteria defined by ACI 363. The 56-day test results reveal that reducing MCAS from 25 mm to 9.5 mm led to an average increase in compressive strength of slightly over 25%.

Several factors contribute to the achievement of higher compressive strength with smaller MCAS: Greater aggregate surface area (Neville, 2011), lower stress concentration around particles (ACI Committee 363, 2010), and a thinner interfacial transition zone at the aggregate-cement paste interface. Smaller aggregates also tend to have fewer internal flaws, like microcracks (Price, 2003), resulting in good mechanical performance, which is favorable for attaining high concrete compressive strength (Caldarone, 2009).

Based on the HSC definitions outlined in the introduction, both CG and CL demonstrate suitability for HSC production. This can be achieved by limiting the MCAS to 12.5 mm or smaller, thereby eliminating the need for supplementary cementitious materials typically used in HSC production. This approach to HSC production offers significant economic advantages for countries that lack access to by-products such as fly ash and silica fume.

Both ACI 211.4R-08 and ACI 363R-10 state that crushed and natural aggregates are acceptable for HSC production, with crushed aggregates generally being more effective due to their ability to create a better bond with the cement paste. The codes also state that HSC can be produced using MCAS of up to 25 mm, but they recommend smaller sizes, preferably 13 mm or less. However, our findings show that only crushed aggregates with an MCAS of 12.5 mm are suitable for HSC production. It should be noted that the present study only

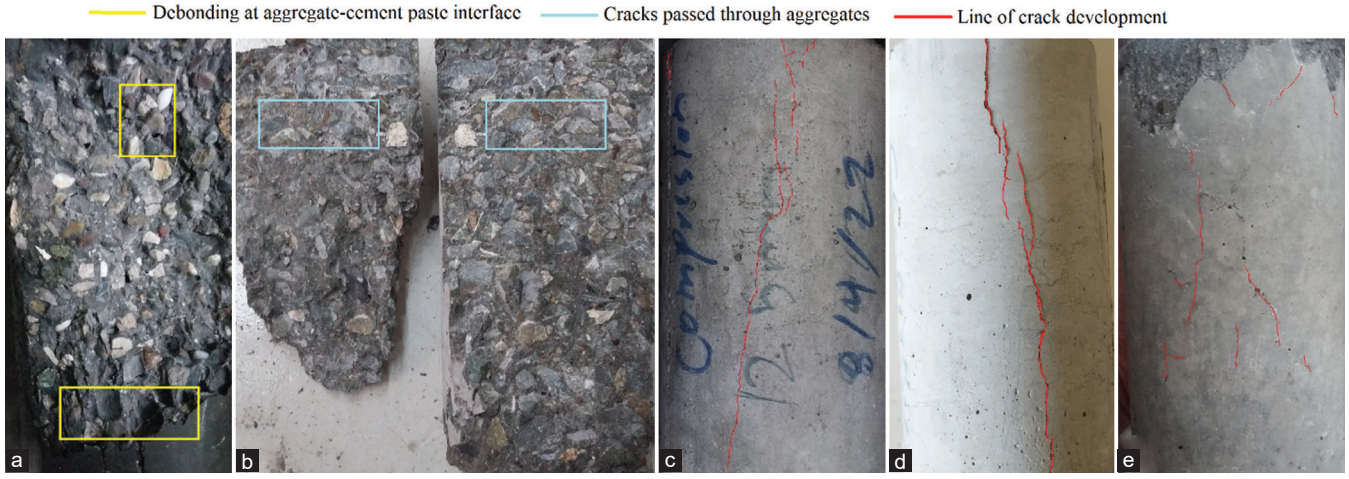

Fig. 7. Failure modes of tested concrete specimens: (a) Crushed gravel, (b) crushed limestone, (c) dolomitic limestone, (d) high-calcite limestone, and (e) natural gravel.

considered cement as the binder for HSC production, while these codes typically consider a combination of cement and supplementary cementitious materials.

C. Splitting Tensile Strength

Fig. 9 presents the results of splitting tensile strength tests conducted on concrete specimens made with different types of aggregates and tested at 7, 28, and 56 days. As expected, the splitting tensile strength increased as the curing duration increased. It is observed that CL concrete recorded the highest splitting tensile strength across all curing periods, followed by DL, CG, HCL, and NG concrete. At 56 days, CL exceeded DL, CG, HCL, and NG by 10.08%, 11.31%, 12.55%, and 18.1%, respectively. These results emphasize the impact of aggregate type on the splitting tensile strength of concrete.

Several researchers (Kılıç et al., 2008; Beushausen and Dittmer, 2015; Vishalakshi, Revathi and Sivamurthy Reddy 2018) have reported that the influence of aggregate type on the compressive strength and splitting tensile strength in HSC is comparable. However, a comparison of the test results presented in Fig. 5 in the previous section and Fig. 9 contradicts this statement. The order of tested concrete specimens, in terms of splitting tensile strength from highest to lowest, was CL, DL, CG, HCL, and NG. In contrast, the order of tested specimens in relation to compressive strength, from highest to lowest, was CG, CL, DL, HCL, and NG.

It is worth noting that there was an exchange of positions between CG and both CL and DL regarding splitting tensile strength. This could be related to the presence of certain particles in CG aggregate that retained a smooth surface texture, which is not desirable for a good mechanical bond between the cement paste and aggregate particles. This observation is supported by Neville (2011), who stated that the tensile strength of low water-to-cement concrete is greatly affected by variations in aggregate surface texture, as the aggregate-cement paste bond controls the tensile strength. The presence of smooth surface texture particles in CG aggregate can influence the compressive strength mainly by affecting the aggregate-cement paste bond. However, the extent of this influence may not be significant in the case of compressive strength results, as concrete made of CG still provided the highest compressive strength value compared to other aggregate types. This might be due to other factors, like aggregate strength, that could play a more dominant role than the surface texture of the aggregates.

Fig. 10 represents the splitting tensile test results of concrete specimens composed of CG with varying MCAS (9.5 mm, 12.5 mm, 19 mm, and 25 mm) and most cured for 7, 28, and 56 days. The results indicate that the splitting tensile strength of concrete decreases as MCAS increases. This trend is similar to the outcomes of the MCAS effect on compressive strength discussed in the previous section, see Fig. 6. Akçaoğlu, Tokyay and Çelik (2004) reported similar results, suggesting that the noted reduction in splitting tensile strength as MCAS increases, corresponds to a decrease in the strength of the aggregate-cement paste bond. Larger aggregate sizes increase the volume of aggregate in relation to cement paste, leading to a greater difference between the elastic moduli of the two constituent phases. This results in greater stress concentration and more microcracks around the aggregates.

D. Relationship between Compressive Strength and Splitting Tensile Strength of HSC

The splitting tensile strength of specimens, incorporating various types and sizes of coarse aggregates and moist-cured at different ages, is graphically presented against the compressive strength results of concrete in Fig. 11. The data shown in Fig. 11 exhibits a notable degree of dispersion, especially beyond a compressive strength of 50 MPa, emphasizing the influence of various aggregate characteristics (types, sizes, shapes, surface texture, and mineralogy) and curing time on the strength behavior of HSC.

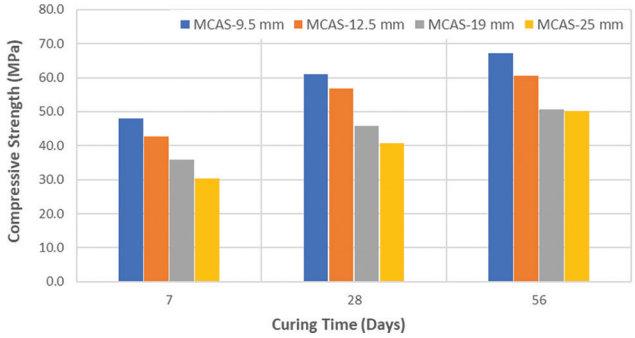

Fig. 8. Effect of various maximum coarse aggregate sizes on the compressive strength of HSC.

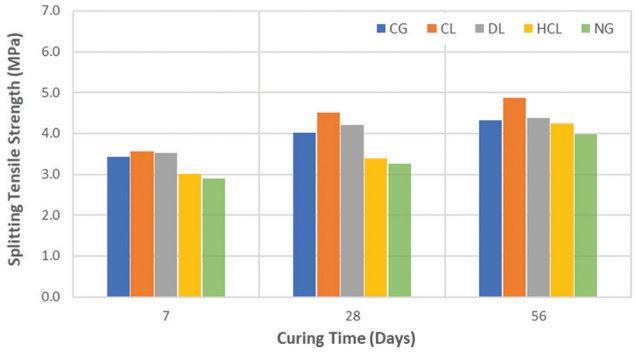

Fig. 9. Effect of aggregate type on the splitting tensile strength of HSC.

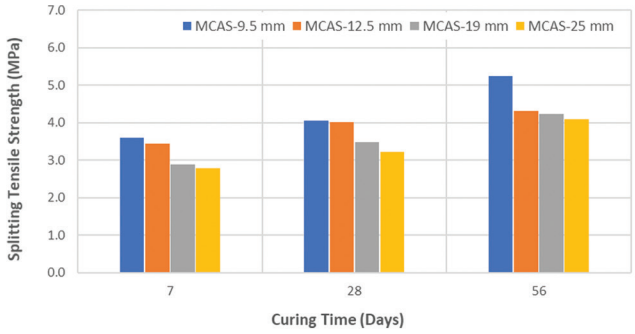

Fig. 10. Effect of various MCAS on the splitting tensile strength of HSC.

http://dx.doi.org/10.14500/aro.11589

Several empirical equations are available to predict splitting tensile strength based on concrete compressive strength. For instance, (ACI Committee 363, 2010) and (ACI Committee 318, 2015) adopted (1) and (2), respectively.

$$f_{ct} = 0.59\sqrt{f_c'} \quad (1)$$

$$f_{ct} = 0.56\sqrt{f_c'} \quad (2)$$

Where f_{ct}: concrete tensile strength, MPa and f_c': concrete compressive strength, MPa

However, the data from this study indicate that both equations seem to overestimate splitting tensile strength for compressive strengths below 50 MPa. Conversely, at higher strengths, they tend to underestimate splitting tensile strength values, as shown in Fig. 9. This result is consistent with the statement that the estimated values of splitting tensile strength using square root equations deviate from experimental splitting tensile strength results as concrete compressive strength increases (Rashid, Mansur and Paramasivam 2002; ACI Committee 363, 2010). In addition, concerns about accuracy and reliability may have factored into the ACI 318 committee's decision to remove (2) from the 2019 edition of ACI 318M.

The majority of researchers (Rashid, Mansur and Paramasivam 2002; Zain et al., 2002; Pul, 2008) who investigated the correlation between compressive strength and tensile strength of concrete predominantly employed the coefficient of determination R^2 as a measure of accuracy for their equation and compared their results with those formulas presented in building standards or developed by previous scholars. However, in contrast to this prevailing approach, the authors of this study believed that the use of other error metrics such as root mean square error (RMSE), mean absolute percentage error (MAPE), and mean square error (MAE) can provide invaluable insights into the performance and accuracy of the equation under development. These metrics can be computed using (3) to (6) (Erdal, Karakurt and Namli 2013; Golafshani, Behnood and Arashpour 2020; Nguyen et al., 2022):

$$R^2 = 1 - \frac{\sum_{i=1}^{n}(y_i - \hat{y}_i)^2}{\sum_{i=1}^{n}(y_i - \bar{y})^2} \quad (3)$$

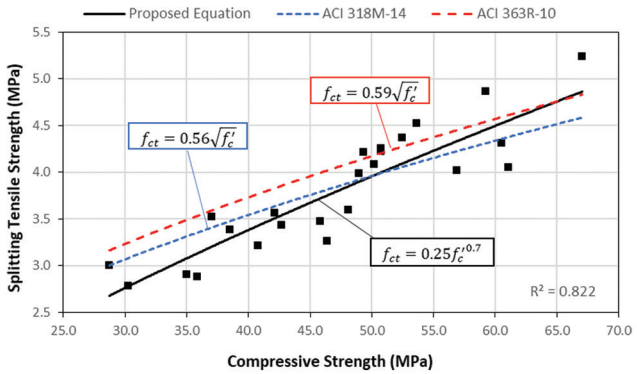

Fig. 11. Comparison between the experiment results (i.e., rectangular shape) and the prediction of splitting tensile strength based on the compressive strength of concrete for different equations.

$$RMSE = \sqrt{\frac{\sum_{i=1}^{n}(y_i - \hat{y}_i)^2}{n}} \quad (4)$$

$$MAPE = \frac{1}{n}\sum_{i=1}^{n}\left|\frac{y_i - \hat{y}_i}{y_i}\right| * 100 \quad (5)$$

$$MAE = \frac{1}{n}\sum_{i=1}^{n}|y_i - \hat{y}_i| \quad (6)$$

Where y_i: observed compressive strength value, $\hat{y}_i$: Predicted compressive strength value, $\bar{y}$: mean of the observed compressive strength values, and n: number of average tests.

In light of the preceding discussion, we introduce a new equation to estimate the splitting tensile strength of concrete based on its compressive strength, as presented in Fig. 9. The data in the present study are divided into two sets: 70% serves as a training dataset for model generation, while the remaining 30% constitutes the testing dataset for model validation. To assess the accuracy of the proposed equation, key error metrics such as R^2, RMSE, MAPE, and MAE were calculated for both the developed equation and those presented in (ACI Committee 363, 2010) and (ACI Committee 318, 2015) for comparison, see Table IV. The results demonstrate that the proposed formula outperforms both equations, with superior accuracy across all metrics. Interestingly, the ACI 363R-10 equation exhibits the lowest performance, underscoring the potential inaccuracy of conventional 0.5-power equations at higher concrete strengths.

For further generalization of the proposed equation, a dataset has been carefully compiled from pertinent literature (Al-Oraimi, Taha and Hassan 2006; Pul, 2008; Beushausen and Dittmer, 2015; Vishalakshi, Revathi and Sivamurthy Reddy 2018; Góra and Piasta, 2020). The compiled compressive strength data are plotted against splitting tensile strength, as depicted in Fig. 12. It is noticeable that the proposed equation provides a better estimation of splitting tensile strength, especially at higher compressive strengths. This observation underscores the potential of the developed equation to provide more reliable predictions in cases of high compressive strengths. The graphical representation in Fig. 12 visually supports and reinforces this noteworthy finding.

Fig. 13 shows the splitting tensile strength residuals of the proposed, ACI 363R-10, and ACI 318-15 equations. The

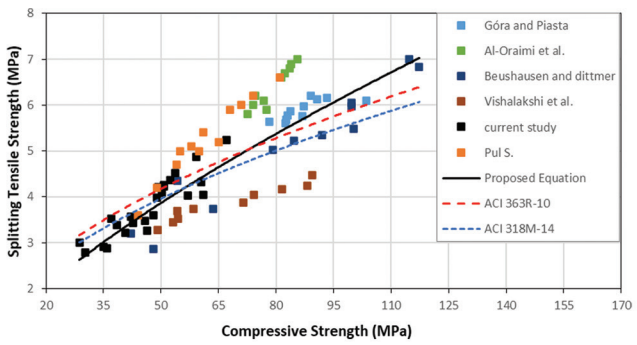

Fig. 12. Performance of the proposed equation, ACI 363R-10, and ACI 318M-14 to predict splitting tensile strength.

TABLE IV
EVALUATION RESULTS OF PROPOSED, ACI 363R-10, ACI 318M-14 EQUATIONS

References	Equations	R^2	RMSE	MAPE	MAE
Proposed Equation	$f_{ct} = 0.25 f_c'^{0.7}$	0.823	0.287	6.231	0.243
(ACI Committee 363, 2010)	$f_{ct} = 0.59\sqrt{f_c'}$	0.810	0.485	13.537	0.472
(ACI Committee 318, 2015)	$f_{ct} = 0.56\sqrt{f_c'}$	0.817	0.377	9.216	0.334

residual plot serves to illustrate the discrepancies between the actual and predicted values within the regression model. The plot features blue, orange, and gray points, which denote the residuals, while the red line signifies the zero-residual axis. Analyzing this plot necessitates consideration of three primary aspects: random scatter, patterns and trends, and heteroscedasticity. The following points provide a detailed examination of these aspects:

1. Random scatter: The residuals exhibit a random scatter around the horizontal axis (represented by the red line). This randomness suggests that the regression model provides an unbiased estimation of the dependent variable, as there is no discernible structure in the residuals.
2. Patterns and trends: The absence of specific patterns, such as curves or linear trends within the residual plot, implies that the chosen regression model is appropriate. A lack of discernible patterns indicates that the model does not suffer from specification errors and that it captures the underlying relationship between the variables effectively.
3. Heteroscedasticity: The uniform spread of residuals across the range of predicted values indicates homoscedasticity, meaning the variance of residuals is constant. This uniformity is crucial for the validity of the model's inferences, as heteroscedasticity could lead to inefficient estimates and affect the reliability of hypothesis tests.

In summary, the analysis of the residual plot suggests that the regression model accurately represents the data. The absence of random scatter, specific patterns, and heteroscedasticity supports the validity of the model, indicating that no further adjustments are necessary. This confirms that the regression model is well-suited for predicting the dependent variable based on the given independent variables.

E. Correlation between Aggregate Impact Value (AIV) and Compressive Strength of HSC

Fig. 14 shows the correlation between the AIV of CG, CL, DL, and HCL aggregates and the compressive strength of HSC at 7, 28, and 56 days of curing. A strong relationship between AIV and compressive strength is evident at 28 and 7 days of curing, with coefficient of determination (R^2) values of 0.9147 and 0.8215, respectively. While the correlation weakens at 56 days (R^2=0.6942), AIV remains relevant for early compressive strength assessment. This finding is crucial from a construction standpoint, as AIV can serve as an important criterion for predicting the quality of concrete in terms of compressive strength.

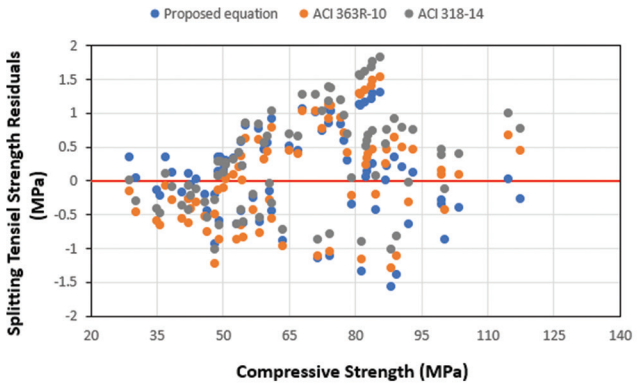

Fig. 13. Splitting tensile strength residual versus compressive of HSC for the proposed, ACI 363R-10, and ACI 318-15 equations.

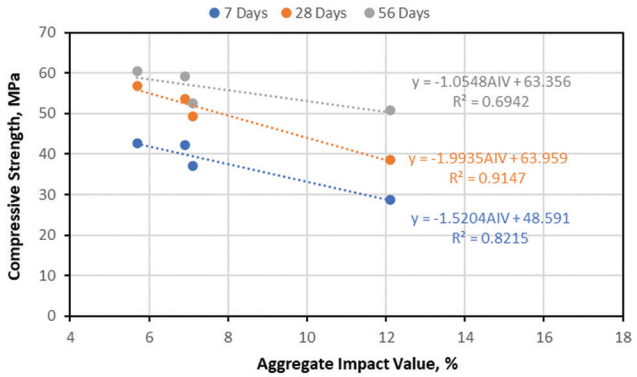

Fig. 14. Correlation between aggregate impact value and compressive strength of HSC.

AIV can be used as a rapid and reliable indicator of aggregate quality that increases the pace of the aggregate selection process. Incorporating AIV into aggregate selection criteria can help ensure that only aggregates with desirable impact values are used, leading to an overall improvement in concrete quality. However, it is important to note that the compressive strength of HSC is influenced by several factors, including aggregate type, size, and surface texture. Therefore, we recommend using AIV in combination with other parameters to provide a more comprehensive assessment of aggregate suitability for HSC production. In addition, further investigation on a wider range of aggregate types, water-cement ratios, and cementitious materials relevant to HSC will refine the AIV-compressive strength relationship, ensuring more reliable and consistent quality control in HSC production.

IV. CONCLUSION

This study investigated the effects of the types and maximum size of coarse aggregate on the mechanical properties of fresh and hardened concrete. In particular, the influence on the compressive strength and splitting tensile strength of HSC toward the optimization of aggregate type and size in concrete mix design for enhanced performance. The following conclusions can be drawn from the key findings of the present study:

1. The MCAS exerts a significant influence on the properties of fresh HSC. The workability of concrete showed an ascending trend as MCAS increased (i.e., increasing MCAS from 9.5 mm to 25 mm led to an increase in slump value from 200 mm to 230 mm). In addition, aggregates characterized by an angular morphology, such as CG, CL, and DL, resulted in a lower slump value compared to rounded-shape and smooth surface NG aggregate.
2. MCAS exerts a pronounced effect on the compressive strength and splitting tensile strength of HSC. Regardless of curing duration, a decrease in MCAS results in an observed increase in both compressive strength and splitting tensile strength of the HSC. Reducing MCAS from 25 mm to 9.5 mm yielded an average increase in compressive strength of slightly over 25%. HSC can be produced using locally available materials by limiting the MCAS of concrete mix to 9.5 mm and 12.5 mm, without the need for supplementary cementitious materials. However, this approach may present certain limitations, such as reducing workability due to a low water-to-cement ratio. This issue can be addressed to a great extent through careful mix design to optimize aggregate size, cement content, and the use of superplasticizers.
3. The compressive strength of concrete produced from CG exceeded that of CL, DL, and HCL aggregates. In contrast, the concrete created with NG aggregate exhibited the lowest compressive strength. This highlights the influence of aggregate type on the performance of HSC. The surface texture of coarse aggregates plays a significant role in influencing the splitting tensile strength of HSC. Among the tested concrete specimens, the ranking in terms of splitting tensile strength, from highest-to-lowest, follows the order of CL, DL, CG, HCL, and NG concrete specimens. However, when considering compressive strength, the sequence was CG, CL, DL, HCL, and NG concrete specimens. Interestingly, for splitting tensile strength, CG traded positions with both CL and DL, despite showing better mechanical properties. This variation may be associated with the presence of smooth surface texture retained by certain particles in NG aggregates, which is not desirable for a good mechanical bond at the aggregate-cement paste interface.
4. Existing empirical equations, such as those from ACI 363R-10 and ACI 318M-14, for predicting tensile strength based on compressive strength show limitations, particularly at high compressive strengths (>55 MPa). A new equation to predict the tensile strength from the compressive strength of HSC is proposed in this study. The evaluation metrics used, including R^2, RMSE, MAPE, and MAE, provided comprehensive insights into the equation's performance, suggesting its potential for more reliable tensile strength prediction in HSC.
5. The correlation between the AIV and compressive strength of HSC is strong at 7 and 28 days of curing, with R^2 of 0.9147 and 0.8215, respectively. However, it moderately weakens at 56 days, with R^2= 0.69. Knowing concrete strength properties through AIV testing is indispensable in practical concrete production.
6. Using locally available materials eliminates the need to import aggregates and supplementary cementitious materials over long distances. This significantly lowers transportation-related energy consumption and carbon emissions, thereby reducing the overall environmental footprint of the construction process. Moreover, sourcing construction materials close to construction sites makes the construction process more flexible and resilient. This is particularly important during global supply chain disruptions, guaranteeing the continuation of construction work without increased costs or delays related to material shortages. The reduction in material costs makes sustainable construction practices more feasible and appealing to local builders and developers.

Although XRF tests were used in this study to determine the chemical composition of aggregate types, a petrographical investigation can provide more detailed results. Therefore, we recommend conducting petrographical analyses in future research to gain a better understanding of the chemical compositions of aggregates. Further studies on the relationship between AIV and the strength properties of HSC concrete can be an interesting topic for researchers.

Acknowledgment

The authors would like to thank Koya University, the Faculty of Engineering, the Civil Engineering Department, and the Concrete Laboratory for supporting us in this study.

References

ACI Committee 211, 2008. *Guide for Selecting Proportions for High-strength Concrete Using Portland Cement and Other Cementitious Materials*. American Concrete Institute, United States.

ACI Committee 318, 2015. *Building Code Requirements for Structural Concrete* (*ACI 318M-14*) *and Commentary* (*ACI 318RM-14*). American Concrete Institute, United States.

ACI Committee 363, 2010. *Report on High-Strength Concrete*. American Concrete Institute, United States.

Akçaoğlu, T., Tokyay, M., and Çelik, T., 2002. Effect of coarse aggregate size on interfacial cracking under uniaxial compression. *Materials Letters*, 57(4), pp.828-833.

Akçaoğlu, T., Tokyay, M., and Çelik, T., 2004. Effect of coarse aggregate size and matrix quality on ITZ and failure behavior of concrete under uniaxial compression. *Cement and Concrete Composites*, 26(6), pp.633-638.

Al-Oraimi, S.K., Taha, R., and Hassan, H.F., 2006. The effect of the mineralogy of coarse aggregate on the mechanical properties of high-strength concrete. *Construction and Building Materials*, 20(7), pp.499-503.

ASTM C127-15, 2015. *Standard Test Method for Relative Density* (*Specific Gravity*) *and Absorption of Coarse Aggregate*. ASTM International, United States.

ASTM C128-15, 2015. *Standard Test Method for Density, Relative Density* (*Specific Gravity*)*, and Absorption of Fine Aggregate*. ASTM International, United States.

ASTM C136/C136M-14, 2014. *Standard Test Method for Sieve Analysis of Fine and Coarse Aggregates*. ASTM International, United States.

ASTM C143/C143M-15a, 2015. *Standard Test Method for Slump of Hydraulic-Cement Concrete*. ASTM International, United States.

ASTM C29/C29M-17a, 2017. *Test Method for Bulk Density* (*Unit Weight*) *and Voids in Aggregate*. ASTM International, United States.

ASTM C33/C33M-18, 2018. *Specification for Concrete Aggregates*. ASTM International, United States.

ASTM C39/C39M-14, 2018. *Standard Test Method for Compressive Strength of Cylindrical Concrete Specimens*. ASTM International, United States.

ASTM C496/C496M-11, 2011. *Standard Test Method for Splitting Tensile Strength of Cylindrical Concrete Specimens*. ASTM International, United States.

ASTM D4791-10, 2010. *Test Method for Flat Particles, Elongated Particles, or Flat and Elongated Particles in Coarse Aggregate*. ASTM International, United States.

Beshr, H., Almusallam, A.A., and Maslehuddin, M., 2003. Effect of coarse aggregate quality on the mechanical properties of high strength concrete. *Construction and Building Materials*, 17(2), p.97.

Beushausen, H., and Dittmer, T., 2015. The influence of aggregate type on the strength and elastic modulus of high strength concrete. *Construction and Building Materials*, 74, pp.132-139.

BS 812-112, 1990. *Testing Aggregates - Method for Determination of Aggregate Impact Value (AIV*).

Caldarone, M.A., 2009. *High-Strength Concrete: A Practical Guide*. 1st ed., CRC Press, London.

Darwin, D., and Dolan, C.W., 2021. *Design of Concrete Structures*. 16th ed., McGraw-Hill Education Asia, United States.

Erdal, H.I., Karakurt, O., and Namli, E., 2013. High performance concrete compressive strength forecasting using ensemble models based on discrete wavelet transform. *Engineering Applications of Artificial Intelligence*, 26(4), pp.1246-1254.

Gjørv, O.E., 2008. 7 - High-strength concrete (Woodhead Publishing series in civil and structural engineering). In: S. Mindess, ed. *Developments in the Formulation and Reinforcement of Concrete*. 2nd ed. Woodhead Publishing, United Kingdom, pp.153-170.

Golafshani, E.M., Behnood, A., and Arashpour, M., 2020. Predicting the compressive strength of normal and High-Performance Concretes using ANN and ANFIS hybridized with Grey Wolf Optimizer. *Construction and Building Materials*, 232, p.117266.

Góra, J., and Piasta, W., 2020. Impact of mechanical resistance of aggregate on properties of concrete. *Case Studies in Construction Materials*, 13, p.e00438.

Grabiec, A.M., Zawal, D., and Szulc, J., 2015. Influence of type and maximum aggregate size on some properties of high-strength concrete made of pozzolana cement in respect of binder and carbon dioxide intensity indexes. *Construction and Building Materials*, 98, pp.17-24.

Jin, L., Yu, W., Li, D., and Du, X., 2021. Numerical and theoretical investigation on the size effect of concrete compressive strength considering the maximum aggregate size. *International Journal of Mechanical Sciences*, 192, p.106130.

Kılıç, A., Atiş, C.D., Teymen, A., Karahan, O., Özcan, F., Bilim, C., and Özdemir, M., 2008. The influence of aggregate type on the strength and abrasion resistance of high strength concrete. *Cement and Concrete Composites*, 30(4), pp.290-296.

Liu, H., Kou, S., Lindqvist, P.A., Lindqvist, J.E., and Åkesson, U., 2005. *Microscope Rock Texture Characterization and Simulation of Rock Aggregate Properties*. *SGU Project 60-1362/2004*. Sveriges Geologiska Undersökning, Sweden. Available from: https://urn.kb.se/resolve?urn=urn: nbn:se: ltu:diva-25098 [Last accessed on 2023 Oct 11].

Meddah, M.S., Zitouni, S., and Belâabes, S., 2010. Effect of content and particle size distribution of coarse aggregate on the compressive strength of concrete. *Construction and Building Materials*, 24(4), pp.505-512.

Neville, A.M., 2011. *Properties of Concrete*. 5th ed., Pearson, Harlow.

Neville, A.M., and Brooks, J.J., 2010. *Concrete Technology*. 2nd ed., Prentice Hall, Harlow.

Nguyen, N.H., Abellán-García, J., Lee, S., Garcia-Castano, E., and Vo, T.P., 2022. Efficient estimating compressive strength of ultra-high performance concrete using XGBoost model. *Journal of Building Engineering*, 52, p.104302.

Price, B., 2003. High strength concrete. In: J. Newman and B. S. Choo, eds. *Advanced Concrete Technology, Process*. Butterworth-Heinemann, Oxford, pp.1-16.

Pul, S., 2008. Experimental investigation of tensile behaviour of high strength concrete. *Indian Journal of Engineering and Materials Sciences*, 15, pp.467-472.

Rao, G.A., and Prasad, B.K.R., 2002. Fracture energy and softening behavior of high-strength concrete. *Cement and Concrete Research*, 32(2), pp.247-252.

Rashid, M.A., Mansur, M.A., and Paramasivam, P., 2002. Correlations between mechanical properties of high-strength concrete. *Journal of Materials in Civil Engineering*, 14(3), pp.230-238.

Uddin, M.T., Mahmood, A.H., Kamal, M.R.I., Yashin, S.M., and Zihan, Z.U.A., 2017. Effects of maximum size of brick aggregate on properties of concrete. *Construction and Building Materials*, 134, pp.713-726.

Vishalakshi, K.P., Revathi, V., and Sivamurthy Reddy, S., 2018. Effect of type of coarse aggregate on the strength properties and fracture energy of normal and high strength concrete. *Engineering Fracture Mechanics*, 194, pp.52-60.

Wu, K., Chen, B., and Yao, W., 2001a. Study of the influence of aggregate size distribution on mechanical properties of concrete by acoustic emission technique. *Cement and Concrete Research*, 31(6), pp.919-923.

Wu, K.R., Chen, B., Yao, W., and Zhang, D., 2001b. Effect of coarse aggregate type on mechanical properties of high-performance concrete. *Cement and Concrete Research*, 31(10), pp.1421-1425.

Zain, M.F.M., Mahmud, H.B., Ilham, A., and Faizal, M., 2002. Prediction of splitting tensile strength of high-performance concrete. *Cement and Concrete Research*, 32(8), pp.1251-1258.